CrossMark

REVIEW

^{11}C-methionine PET/CT findings in benign brain disease

Reiko Nakajima[1] · Ken Kimura[1] · Koichiro Abe[1] · Shuji Sakai[1]

Abstract ^{11}C-methionine (MET) is one of the most commonly used positron emission tomography (PET) tracers for evaluation of malignant brain tumor, with MET-PET being a sensitive technique for visualization of primary and recurrent malignant brain tumors. However, previous reports have demonstrated MET uptake in lesions associated with benign brain diseases. These diseases usually show an increase in MET uptake similar to that of malignant tumors. This pitfall in MET-PET image interpretation is important not only for nuclear medicine professionals, but also for radiologists. In this review, we demonstrate the imaging characteristics of MET uptake in benign brain disease, and recommend physician interpretation of imaging findings and disease characteristics for optimal patient management. Benign uptake must be identified to prevent misdiagnosis and unnecessary surgical operations.

Keywords ^{11}C-methionine (MET) · Positron emission tomography (PET) · Benign brain disease

Introduction

^{11}C-methionine (MET) is among most popular amino acid tracers for the positron emission tomography (PET) imaging of brain tumors. MET-PET/computed tomography (CT) imaging is a sensitive technique, and the roles of MET-PET imaging in the work-up of primary gliomas include diagnostic accuracy, tumor grading, prognosis, assessment of therapeutic response, assessment of tumor extent, biopsy, and radiotherapy planning, while it also valuable for differentiating between tumor recurrence and radiation necrosis in brain metastases. Brain tumor uptake on MET images can be affected by amino acid transport (sodium-independent L-transporter, LAT1, 2, and 3), MET metabolism, tumor vascular bed-dependent blood flow, microvessel density, and blood–brain barrier (BBB) distribution [1–3]. The accumulation of MET through these mechanisms is visualized as tissue uptake on PET images, with MET being incorporated into most brain tumors, including low-grade gliomas. In general, MET uptake is lower in low-grade than in high-grade gliomas, although there is considerable overlap between these two groups, as well as between histological types [4, 5]. However, several previous reports have demonstrated MET uptake in lesions associated with benign brain diseases [6–23]. Although Ito et al. [6] have already reported on the imaging spectrum and pitfalls of MET-PET/CT in intracranial lesions, in this review we focus on and introduce imaging characteristics of MET uptake in benign brain disease through a literature review. We recommend physician interpretation of imaging findings and disease characteristics for optimal patient management. Benign uptake must be identified to prevent misdiagnosis and unnecessary surgical operations. These pitfalls in MET-PET image interpretation are important not only for nuclear medicine professionals, but also for radiologists.

Methods for the assessment of MET-PET images

Many reports have made visual assessments and semiquantitative evaluations of MET-PET/CT. The visual assessment of MET-PET images is straightforward and easy.

✉ Reiko Nakajima
  nakajima.reiko@twmu.ac.jp

1   Departments of Diagnostic Imaging and Nuclear Medicine,
    Tokyo Women's Medical University, 8-1 Kawada-cho,
    Shinjuku-ku, Tokyo 162-8666, Japan

Every area of uptake higher than the background (normal grey matter) is considered to be potentially pathological. Semiquantitative evaluation uses the maximal standardized uptake value (SUV_{max}) and the tumor-to-normal tissue ratio (TNR). Whether the SUV itself has a real diagnostic value is still under debate. MET-PET is mainly interpreted by comparing MET uptake in the tumor with that in the corresponding normal region in the contralateral hemisphere or frontal lobe and deriving the TNR. Uda et al. [24] reported on MET uptake in the normal brain and report that frontal or parietal cortex are more appropriate as reference regions than the cerebellum or brain stem, as they demonstrate low coefficients of variations. This is the reason, the most often used calculation method is the TNR, which compares the uptake in the tumor to that in the contralateral frontal lobe. The TNR is calculated as follows:

$$TNR = SUV_{max} \text{ of the tumor lesions/}$$

SUV_{mean} of normal contralateral frontal cortex.

Vascular diseases

Cavernous malformation

Cavernous malformation is a relatively common vascular malformation that is usually found incidentally on magnetic resonance (MR) imaging. A cavernous malformation is a vascular hamartoma composed of variably sized interpapillary vascular spaces, sinusoids, and larger cavernous spaces without intervening brain tissue. These lesions lack smooth muscle support and are filled with blood or thrombus. Regardless of the overt hemorrhage status, cavernous malformations are associated with hemosiderin, which may be related to absent or diminished tight junctions seen in ultrastructural studies. This implies a localized loss of the BBB and diminished vascular stability [25], which is indicated by increased MET uptake within a cavernous malformation (Fig. 1). Although there have been no previous reports on MET-PET of intracranial cavernous malformations, Naito et al. [26], reported on a cavernous malformation in the spinal cord. According to their report, MET-PET showed weak to moderate MET accumulation in the cavernous malformation in the spinal cord, with the SUV_{max} values of the lesions being 1.377 and 3.54 [26].

Venous infarction

Venous infarction had been considered more likely than brain malignant tumor using the enhanced MR imaging. In a case report, Harada et al. [7] reported that MET/PET imaging revealed a higher MET uptake in the lesion than in the surrounding cortex, with a TNR of 1.69. Because of the increased MET uptake in the venous infarction, their MET-PET/CT findings were consistent with those of low grade glioma (Fig. 2). However, MET-PET/CT imaging for venous infarction also yields false-negative results. The mechanism of MET uptake is breakdown of the BBB and infarction, which are the potential mechanisms underlying the positive MET findings. Venous infarction has several risk factors, with oral contraceptive drug use and pregnancy being well-known causes of thrombosis in young women. Other risk factors for venous infarction are prothrombotic conditions (either genetic or acquired), infection, and malignancy.

Cerebral infarction

High MET uptake has also been reported with cerebrovascular diseases (CVDs) such as cerebral infarction [8–11]. Nakagawa, et al. [8] reported that the mean MET uptake in cerebral infarctions was 1.07 ± 0.28 (range 0.67–1.31) the TNR, with this value depending on the day of onset. The mechanism of MET uptake is via the infiltration of inflammatory cells, and gliosis is considered to play an important role in the high MET uptake observed in cerebral infarctions. BBB breakdown associated with infarction causes leakage of MET into the extracellular space, thus enabling high cellular uptake under certain conditions, with modification of amino acid transport. Increased blood flow is likely to modify the transport mechanism, resulting in high MET uptake.

Hematoma

Neoplastic or non-neoplastic hemorrhages are not unusual. When treating patients with intracerebral hemorrhage, it is important to accurately diagnose the etiology, because of the specific management. Nakagawa, et al. [8] reported that mean MET uptake in the periphery of hematomas was 1.12 ± 0.04 (range 1.10–1.17) the TNR. However, Dethy et al. [12] reported that high uptake of MET in the area surrounding a hematoma showed a dramatic reduction or disappearance after the bleeding. Ogawa et al. [13] reported that compared with CT or MR, MET-PET could distinguish neoplastic from non-neoplastic hematomas according to differences in lesion extent. According to their study [13], MET-PET showed increased accumulation in the regions around non-neoplastic hematomas in the subacute stage; however, there was no accumulation in acute stage non-neoplastic hematomas. In both acute and subacute stage neoplastic hematomas, MET-PET showed increased accumulation of MET in a large area around lesions, beyond that showing enhancement on CT or MRI.

As mentioned above, the mechanism is the same as in cerebral infarction, with BBB breakdown associated with infarction causing leakage of MET into the extracellular space, thus enabling high cellular uptake under certain
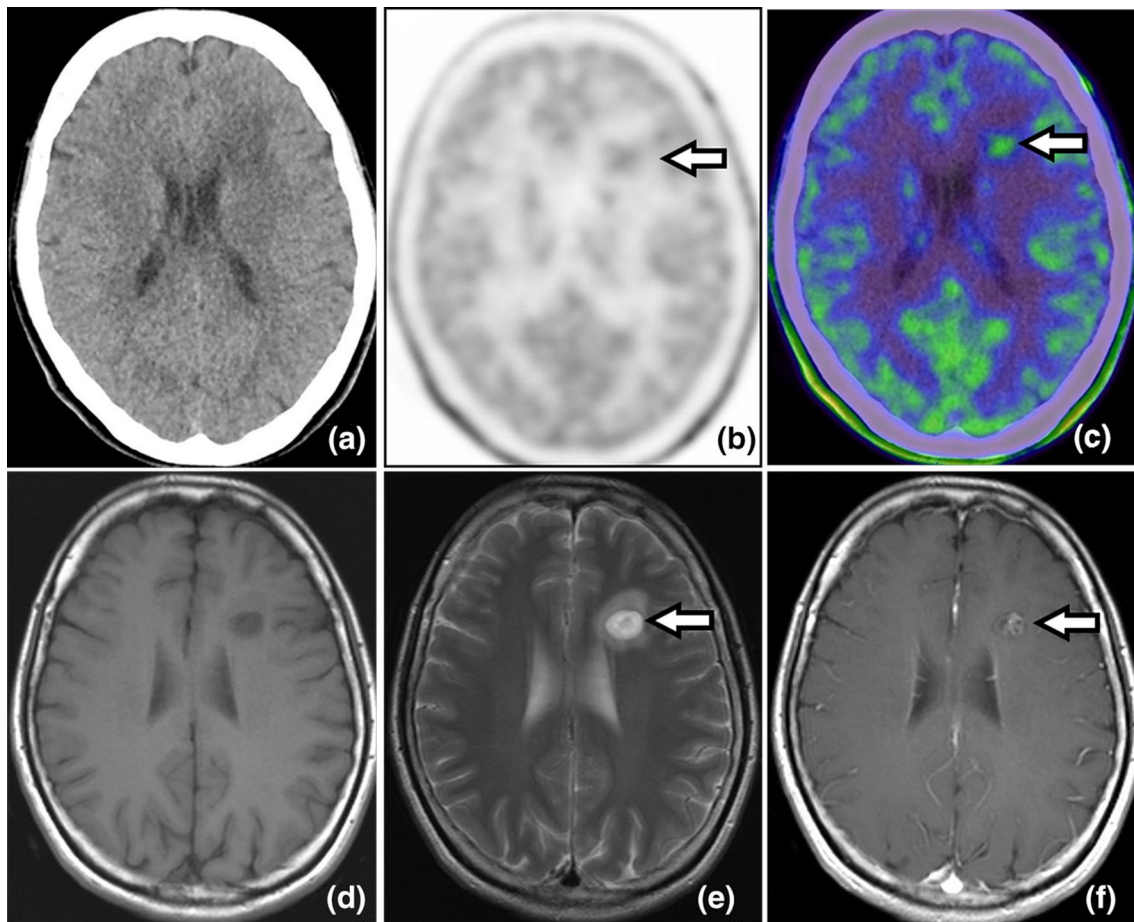
Fig. 1 **a** CT shows a hypodensity in the left frontal lobes. **b** MET-PET and **c** PET/CT images show mild uptake corresponding to the lesion (arrows), with a maximum standard uptake value (SUV$_{max}$) of 1.78 and a TNR of 1.5. **d** T1-weighted imaging (WI) and **e** T2-WI respectively show a low and high intensity mass, which shows enhancement (*arrows*) on Gd-T1WI (**f**). We diagnosed a cavernous malformation according to the radiological findings

conditions, and modification of amino acid transport. The uptake of MET is also related to the protein synthesis rate, which is increased in inflammatory cells or proliferating glial cells [27]. Therefore, the high uptake of MET observed may be related to the cellular reactions surrounding the hematoma. Increased blood flow will likely modify the transport mechanism, resulting in high MET uptake (Fig. 3).

Benign brain tumors

Meningioma

Meningiomas, which are usually benign, are the most common type of brain tumor (Figs. 4, 5). Malignant meningiomas (WHO grade II or III) have a worse prognosis than WHO grade I meningiomas. However, Arita et al. [14] reported that the mean and maximum MET TNR did not differ significantly between benign and malignant meningiomas (WHO grade I: TNR = 2.45 ± 0.67, WHO grade II: TNR = 2.13 ± 0.63). Although TNR is significantly higher for symptomatic and skull-base meningiomas than for non-symptomatic and non-skull-base tumors, MET uptake does not correlate with tumor aggressiveness (MIB-1 index, tumor-doubling time, tumor grade) [14].

The biological factors that affect MET uptake in meningiomas and provide fundamental information for MET-PET interpretation have not yet been fully examined, although Arita et al. [14] reported that MET uptake could be affected by cerebral blood volume (CBV) within the tumor (Figs. 4, 5).

Radiation necrosis

Several studies have indicated the advantages of MET-PET/CT for distinguishing radiation necrosis from focal recurrence after radiotherapy. The uptake of MET in recurrence is different from that in radiation necrosis. As
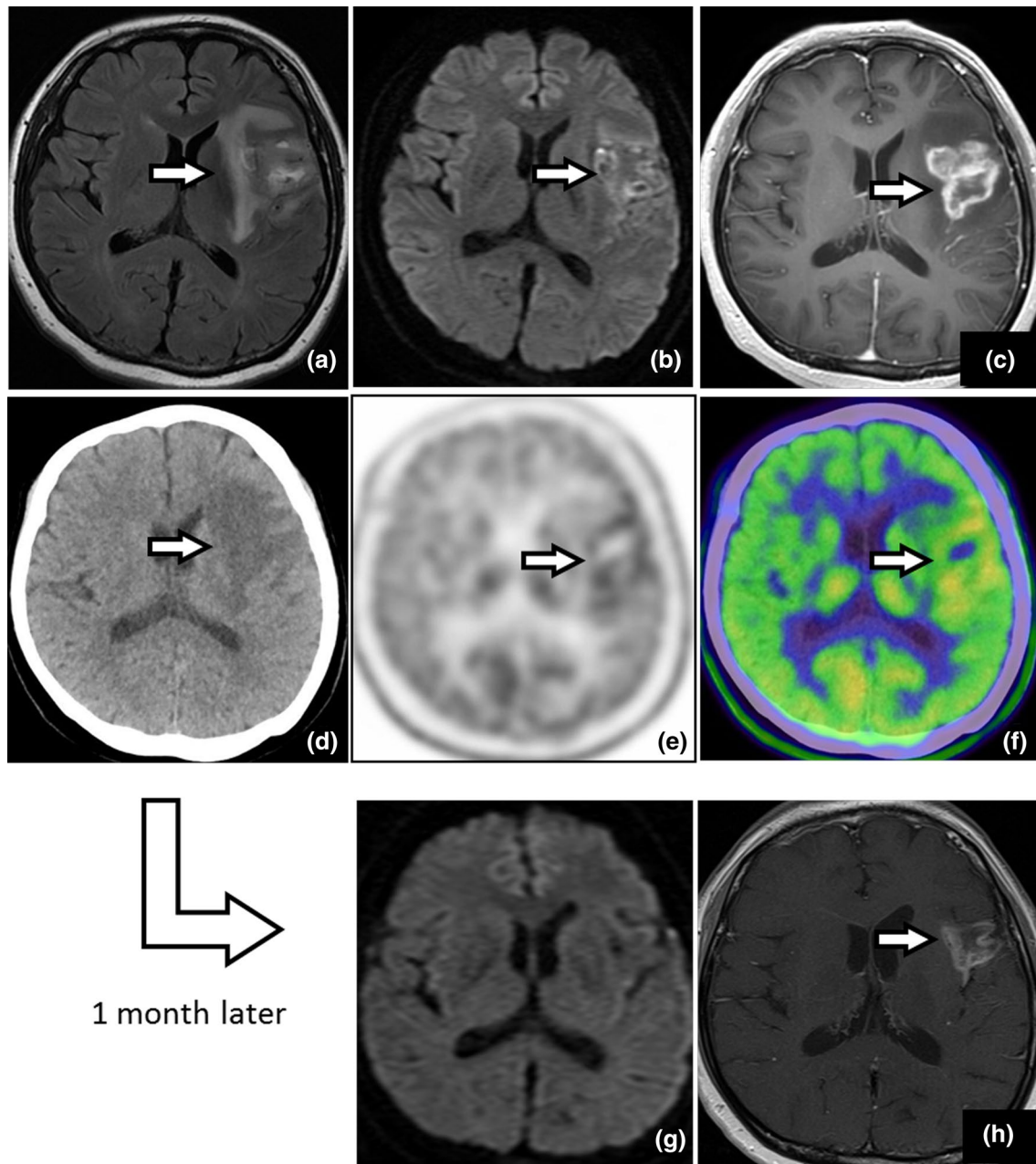
Fig. 2 A 52-year-old woman with a speech impediment. MRI FLAIR (**a**) and DWI images (**b**; day 2) show a high intensity lesion with enhancement on Gd-T1WI (**c**), which is suggestive of a tumor with ring enhanced components, such as a glioblastoma. CT (**d**; day 4) shows a low density lesion in the left frontal lobe. On MET-PET/CT obtained on the same day as CT, MET-PET (**e**) and PET/CT images (**f**) show moderate uptake corresponding to the lesion (*arrows* in primary gliomas, the uptake in recurrent tumor lesions is caused by active uptake of MET by the tumor cells [15, 16]. However, radiation injury occurs in the endothelial cells of small-to-medium-sized arteries. Occlusion of these arteries leads to passive necrosis, diffusion across a broken BBB, and increased angiogenesis. With regard

$SUV_{max} = 3.81$, $TNR = 1.94$ respectively). These PET findings are consistent with those of low-grade glioma. The patient revealed that she had been taking an oral contraceptive drug. Follow-up MR imaging 1 month after onset revealed disappearance of the high intensity lesion on DWI (**g**) and a decreased area of enhancement on Gd-T1WI (**h**). We finally diagnosed a venous infarction

to vascular pathology, reactive gliosis or inflammatory changes can also influence the accumulation of MET in radiation injury [28]. Theoretically, the uptake in tumor cells should exceed the uptake after radiation injury, but there is the possibility of overlap between these mechanisms of uptake (Fig. 6). Previous studies have reported
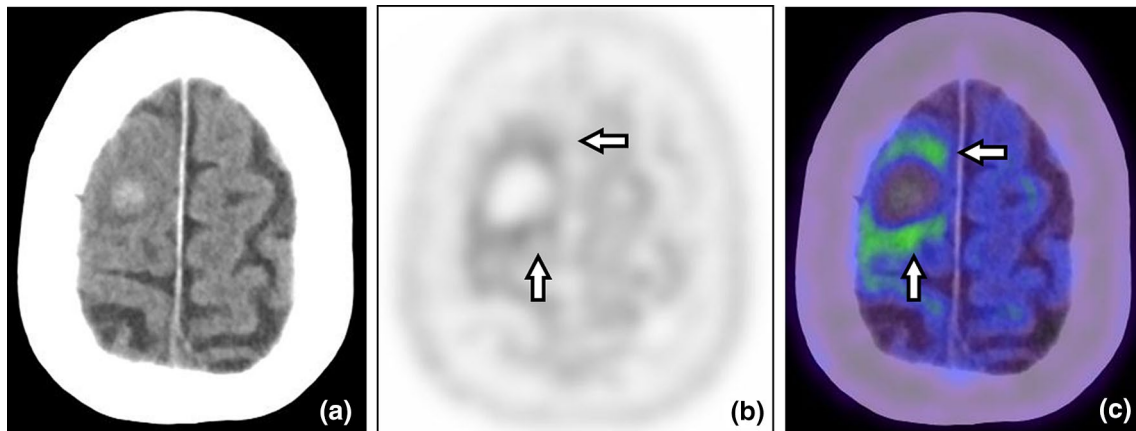
Fig. 3 Hematoma in an 80-year-old woman. Right frontal non-neo-plastic hematoma 20 days after a bleeding episode (chronic stage). CT (**a**) shows a resolving hematoma with surrounding edema. MET-PET (**b**) and PET/CT (**c**) images show low uptake in the subcortical area surrounding an area of slight mild cortical uptake in the right frontal lobe (*arrows*). We diagnosed a non-neoplastic hematoma according to the clinical and radiological findings
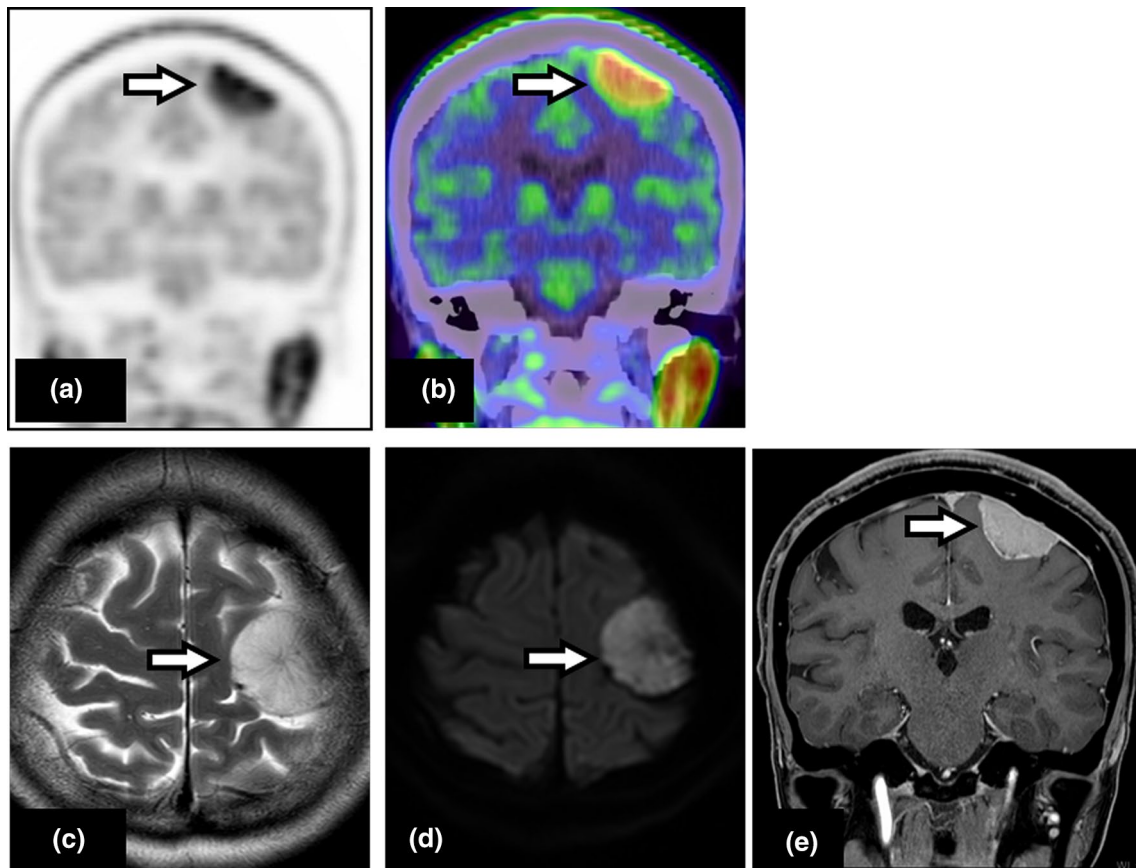

Fig. 4 Meningothelial meningioma (WHO grade I) in a 55-year-old man. MET-PET (**a**) and PET/CT images (**b**) show moderate uptake corresponding to the lesion (*arrows* $SUV_{max} = 5.65$, $TNR = 3.90$, respectively). T2WI (**c**) and DWI (**d**) MRI reveal a high intensity extracranial lesion with homogenous enhancement on Gd-T1WI (**e**), suggesting a typical tumor such as a meningioma. The patient received a histopathological diagnosis of a meningothelial meningioma (WHO grade I)
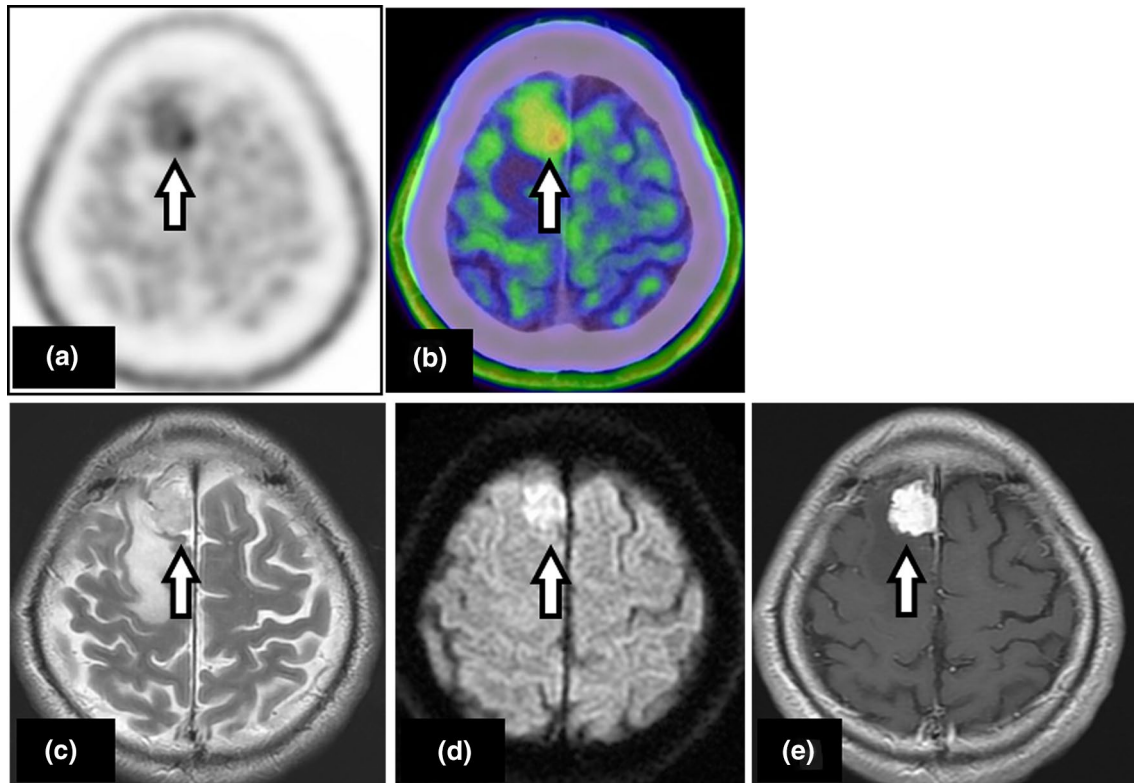
Fig. 5 An angiomatous meningioma (WHO grade I) in a 51-year-old woman. MET-PET (**a**) and PET/CT (**b**) images show moderate uptake corresponding to the lesion (*arrows* SUV$_{max}$ = 4.17, TNR = 2.54, respectively). T2WI (**c**) and DWI (**d**) MRI reveal a high intensity extracranial lesion with homogenous enhancement on Gd-T1WI (**e**), suggesting a typical tumor such as a meningioma. The patient received a histopathological diagnosis of an angiomatous meningioma (WHO grade I)
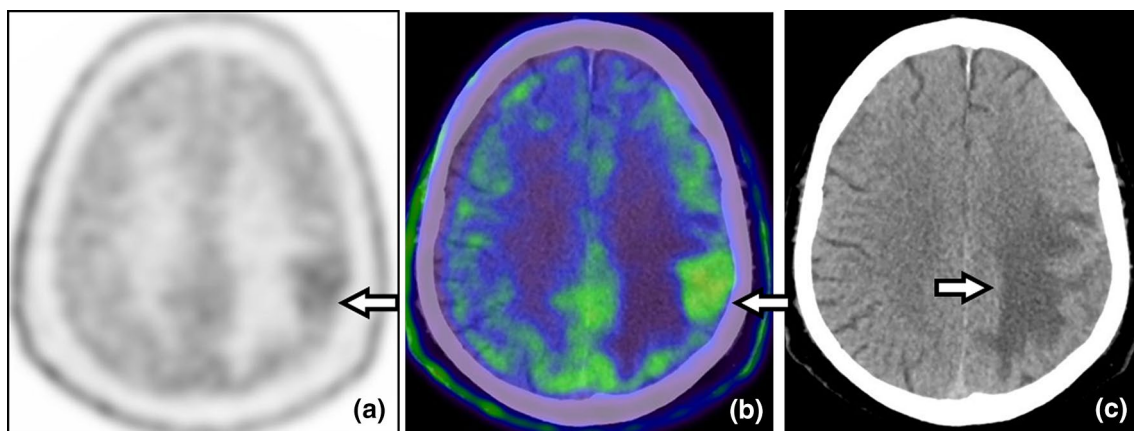

Fig. 6 Radiation necrosis in a 68-year-old man. The patient had previously been treated for lung cancer via tumor resection, and for brain metastatic lesions via radiotherapy. Plane CT obtained 2 years after initial surgery showed a low density area in the left parietal area. MET-PET (**a**) and PET/CT (**b**) images showed slight tracer accumulation corresponding to the CT (**c**) image abnormality. The SUV$_{max}$ and TNR were 2.73 and 1.74 respectively. Gliosis without tumor was pathologically demonstrated through a second surgery

that differences in the TNR cut-off range from 1.27 to 1.9 can be used for differentiation of tumor from radiation necrosis, with studies reporting sensitivities ranging from 75 to 100%, specificities from 60 to 100%, and diagnostic accuracy from 82 to 94% [28]. Terakawa et al. [16] also reported that cut-off values differed between metastatic lesions and gliomas when comparing them with radiation necrosis. They reported that a TNR (SUVmean) of

greater than 1.41 provided the best sensitivity and specificity for metastatic brain tumor (79 and 75% respectively), and that a TNR (SUVmean) of greater than 1.58 provided the best sensitivity and specificity for glioma (75 and 75% respectively) [16].

Demyelinating disease

Multiple sclerosis/tumefactive multiple sclerosis

Multiple sclerosis (MS) causes inflammatory demyelination of the central nervous system. Tumefactive multiple sclerosis (TMS) is a rare variant of MS with tumefactive demyelinating lesions (TDL). The MR imaging findings of TDL are a tumor-like appearance with a size >2 cm, mass effect, and edema. Typical radiographic features of large demyelinating plaques often mimic those of brain tumors (e.g., malignant high-grade gliomas/metastatic brain tumors). A few reports have described mild MET uptake in typical MS [17], and a remarkable MET uptake has been observed in TDL on MET-PET [18, 19]. However, one report described insignificant MET uptake in TMS [29]. Schiepers et al. [30] performed fludeoxyglucose- (FDG)-PET in 13 patients

with MS and found that large lesions in stable MS demonstrate a relatively increased FDG uptake; they considered that the degree of FDG uptake may simply indicate the temporal stage of the demyelinating plaque [30]. MET uptake is also detected during the acute inflammatory phase of MS (Fig. 7).

TMS is a representative disease with various uptake patterns that depend on the disease activity (Fig. 8); uptake is due to increased metabolism and active amino acid transport resulting from the increased density of inflammatory cells, as well as disruption of the BBB. Additionally, MET uptake patterns may not necessarily correspond to the enhancement patterns in lesions.

Infection

Encephalitis

Encephalitis is an acute inflammation of the brain, which is usually caused by a viral infection. Several reports [20–22] have described MET uptake in encephalitis (e.g., Rasmussen syndrome and anti-NMDA [NR2B] receptor
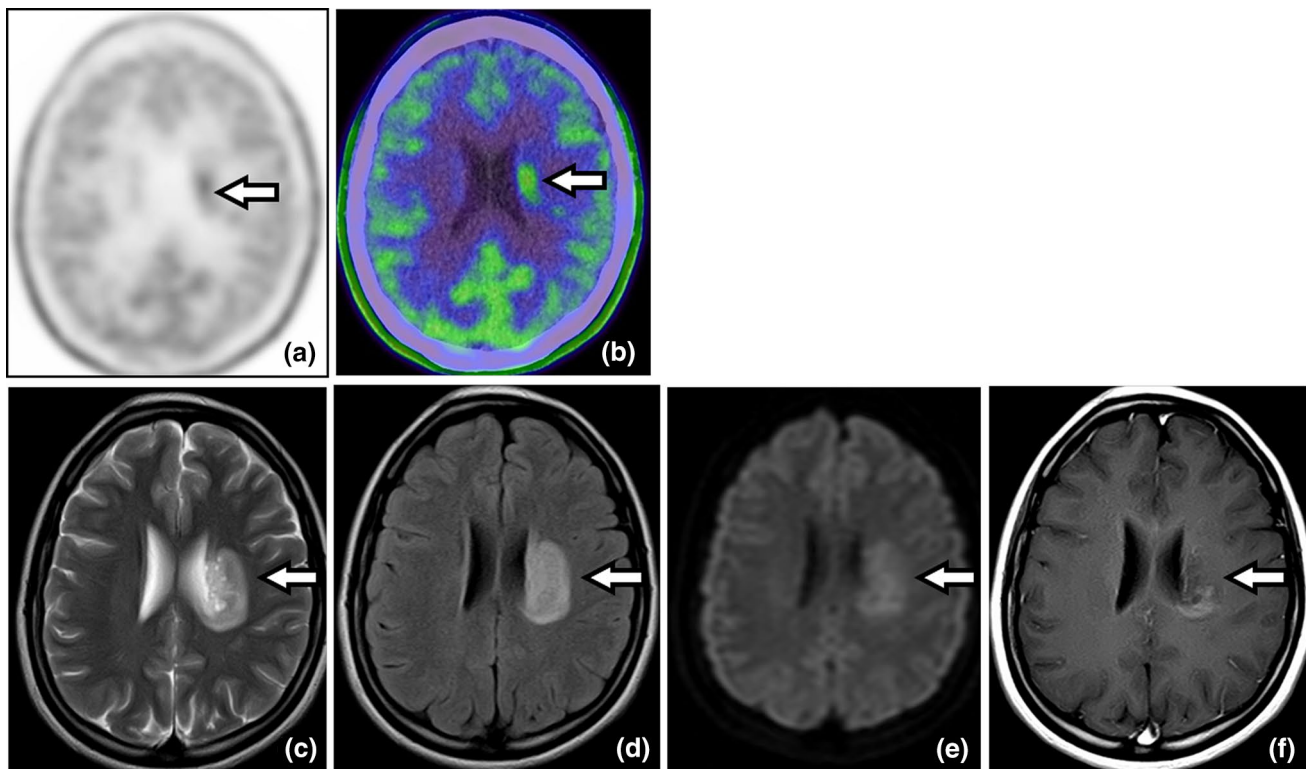

Fig. 7 Multiple sclerosis (MS) in a 31-year-old woman. MET-PET (**a**) and PET/CT (**b**) show moderate uptake corresponding to the lesion (*arrows* SUV_{max} = 2.35, TNR = 1.56, respectively). T2WI (**c**), FLAIR (**d**), and DWI (**e**) MRI performed almost simultaneously with MET-PET/CT show a high intensity lesion with enhancement on Gd-T1WI (**f**), suggesting a tumor with enhanced components (e.g., malignant brain tumor). MET uptake may not correspond with the enhancing areas in the lesions. The patient received a histopathological diagnosis of a multiple sclerosis
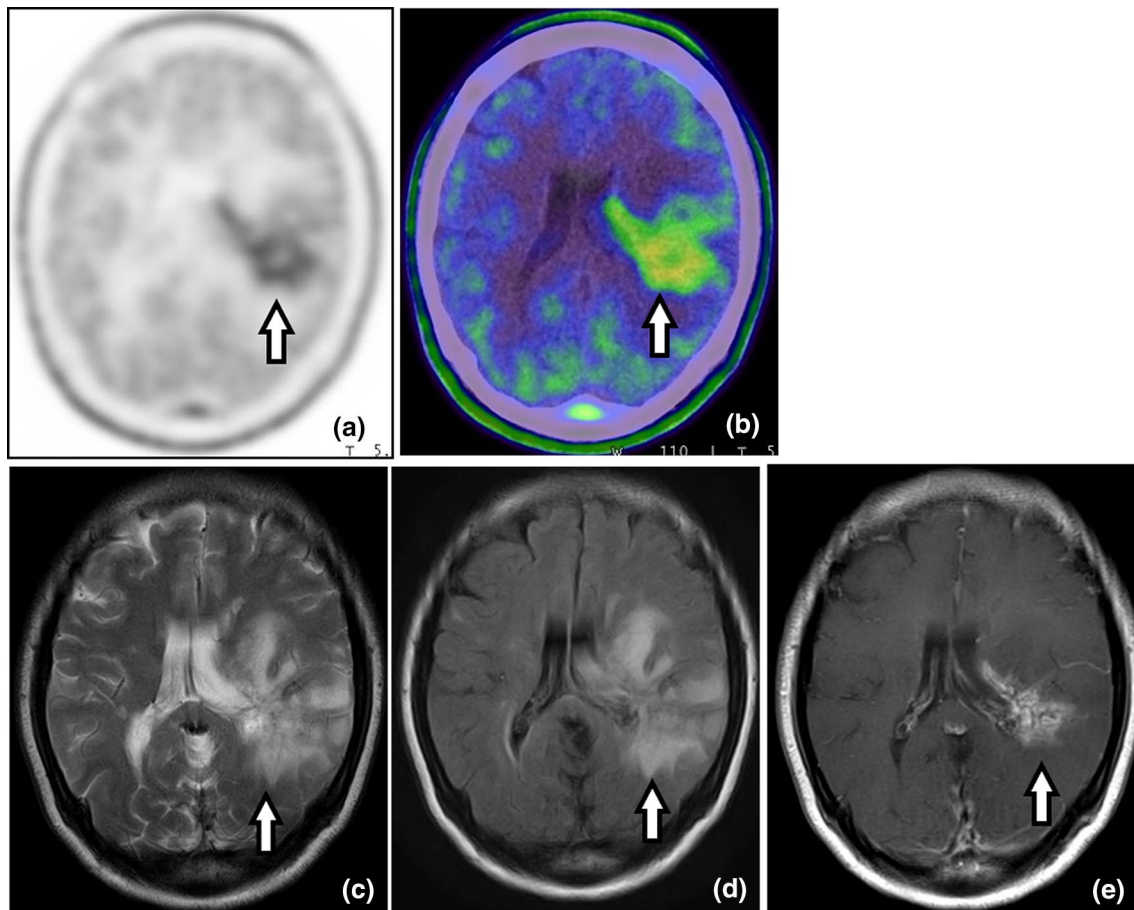
Fig. 8 Tumefactive multiple sclerosis (TMS) in a 19-year-old woman. MET-PET (**a**) and PET/CT (**b**) show remarkable uptake corresponding to the lesion (*arrows* $SUV_{max} = 3.32$, TNR = 2.54, respectively). T2WI (**c**) and FLAIR (**d**) MRI conducted almost simultaneously with MET-PET/CT show a high intensity lesion with enhancement on Gd-T1WI (**e**), suggesting a tumor with enhanced components (e.g., malignant brain tumor). The patient was finally diagnosed with TMS

encephalitis). Encephalitis exhibits various uptake patterns and extents, even when caused by the same pathogen. MET uptake in encephalitis is relatively dependent on disease activity, increased density of inflammatory cells, and amino acid transporter activation.

Brain abscesses

The degree of MET tracer uptake is not associated with a specific type of bacteria. Tsuyuguchi et al. [23] reported that MET-PET studies more directly reflect the degree of inflammatory response in brain abscesses when compared with enhanced CT or MRI. MET-PET is useful for assessing the clinical effects of antibiotic treatments on brain abscesses [23]. Accumulation in brain abscesses may be related not only to disruption of the BBB, but also to an increased density of inflammatory cells (Fig. 9).

Conclusion

We suggest that these benign brain diseases should be added to the list of potential pitfalls regarding MET uptake in brain lesions. It is important for both nuclear medicine
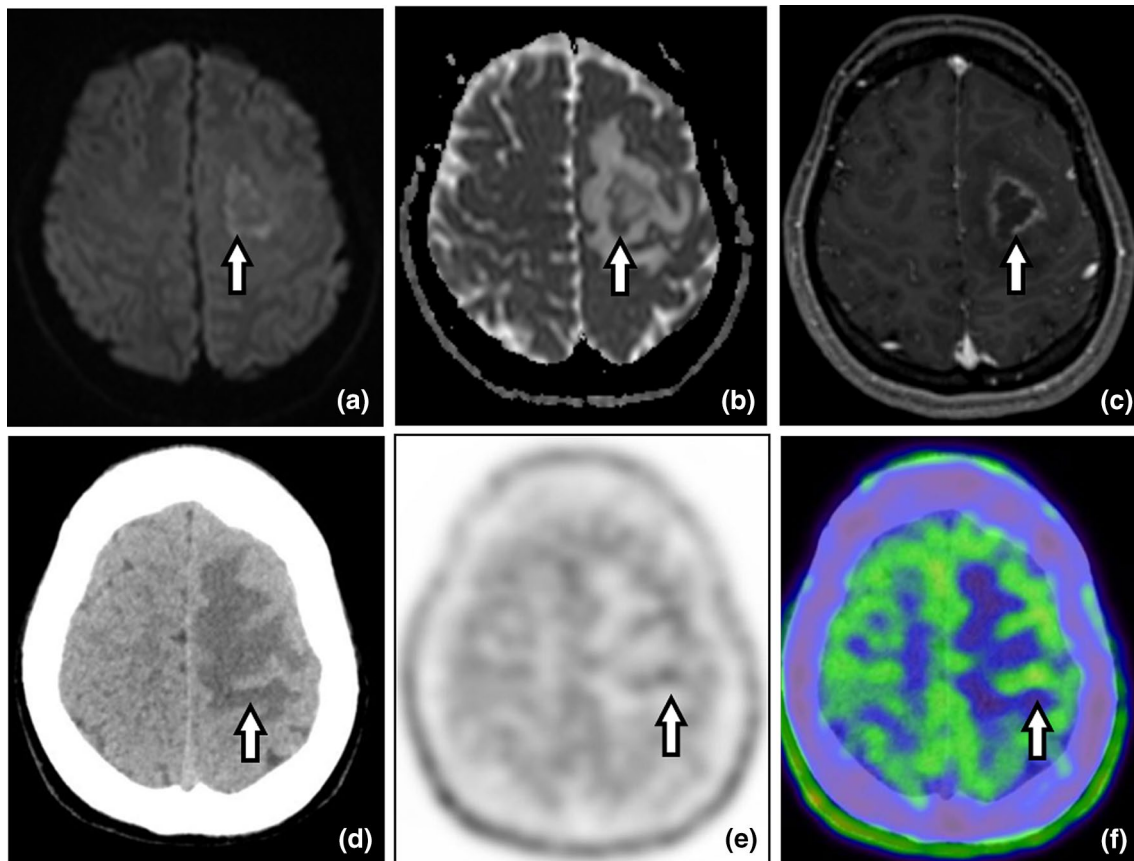
Fig. 9 Brain abscesses in a 19-year-old woman with headache. DWI (**a**) images (day 2) show a weak high intensity lesion and low ADC values (**b**) with ring enhancement and edema on Gd-T1WI (**c**), suggesting a tumor with enhanced components (e.g., malignant brain tumor or brain abscess). After antibiotic treatment, plane CT (**d**; day 9) shows a low intensity lesion. MET-PET and PET/CT images (**e**, **f**; day 9) show weak uptake corresponding to the lesion (*arrows* SUV_{max} = 2.72, TNR = 1.40, respectively). The patient received a histological diagnosis of a brain abscess

professionals and radiologists to be familiar with the features and pitfalls of MET-PET/CT imaging. To prevent misdiagnosis and unnecessary surgical interventions when evaluating cranial lesions, CT, MRI and PET examinations should be combined.

References

1. van Waarde A, Elsinga PH. Proliferation markers for the differential diagnosis of tumor and inflammation. Curr Pharm Des. 2008;14:3326–39.
2. Ishiwata K, Kubota K, Murakami M, Kubota R, Sasaki T, Ishii S, et al. Re-evaluation of amino acid PET studies: can the protein synthesis rates in brain and tumor tissues be measured in vivo? J Nucl Med. 1993;34:1936–43.
3. Omidi Y, Barar J. Impacts of blood–brain barrier in drug delivery and targeting of brain tumors. Bioimpacts. 2012;2:5–22.
4. Shinozaki N, Uchino Y, Yoshikawa K, Matsutani T, Hasegawa A, Saeki N, et al. Discrimination between low-grade oligodendrogliomas and diffuse astrocytoma with the aid of ^{11}C-methionine positron emission tomography. J Neurosurg. 2011;114:1640–7.
5. Kato T, Shinoda J, Nakayama N, Miwa K, Okumura A, Yano H, et al. Metabolic assessment of gliomas using ^{11}C-methionine, [^{18}F] fluorodeoxyglucose, and ^{11}C-choline positron-emission tomography. AJNR. 2008;29:1176–82.
6. Ito K, Matsuda H, Kubota K. Imaging spectrum and pitfalls of (11)C-methionine positron emission tomography in a series of patients with intracranial lesions. Korean J Radiol. 2016;17:424–34.
7. Harada Y, Hirata K, Kobayashi H, Usui R, Shiga T, Terae S, et al. A pitfall of C-11 methionine PET cerebral venous infarction mimicked a glioma. Clin Nucl Med. 2012;37:110–1.
8. Nakagawa M, Kuwabara Y, Sasaki M, Koga H, Chen T, Kaneko O, et al. ^{11}C-methionine uptake in cerebrovascular disease: a comparison with ^{18}F-fDG PET and ^{99m}Tc-HMPAO SPECT. Ann Nucl Med. 2002;16:207–11.

9. Nagano-Saito A, Kato T, Wakabayashi T, Nishino M, Ohshima M, Ito K, et al. High- and moderately high-methionine uptake demonstrated by PET in a patient with a subacute cerebral infarction. Ann Nucl Med. 2001;15:387–91.

10. Jacobs A. Amino acid uptake in ischemically compromised brain tissue. Stroke. 1995;26:1859–66.

11. Mineura K, Sasajima T, Kowada M, Ogawa T, Hatazawa J, Umemura K. Indications for differential diagnosis of nontumor central nervous system diseases from tumors. A positron emission tomography study. J Neuroimaging. 1997;7:8–15.

12. Dethy S, Goldman S, Blecic S, Luxen A, Levivier M, Hildebrand J. Carbon-11-methionine and fluorine-18-FDG PET study in brain hematoma. J Nucl Med. 1994;35:1162–6.

13. Ogawa T, Hatazawa J, Inugami A, Murakami M, Fujita H, Shimosegawa E, et al. Cardon-11-Methionine PET evaluation of intracerebral ematoma: distinguishing neoplastic from non-neoplastic hematoma. JNM. 1995;36:2175–9.

14. Arita H, Kinoshita M, Okita Y, Hirayama R, Watabe T, Ishohashi K, et al. Clinical characteristics of meningiomas assessed by ^{11}C-methionine and ^{18}F-fluorodeoxyglucose positron-emission tomography. J Neurooncol. 2012;107:379–86.

15. Tsuyuguchi N, Sunada I, Iwai Y, Yamanaka K, Tanaka K, Takami T, et al. Methionine positron emission tomography of recurrent metastatic brain tumor and radiation necrosis after stereotactic radiosurgery: is a differential diagnosis possible? J Neurosurg. 2003;98:1056–64.

16. Terakawa Y, Tsuyuguchi N, Iwai Y, Yamanaka K, Higashiyama S, Takami T, et al. Diagnostic accuracy of ^{11}C-methionine PET for differentiation of recurrent brain tumors from radiation necrosis after radiotherapy. J Nucl Med. 2008;49:694–9.

17. Faria Dde P, Copray S, Buchpiguel C, Dierckx R, de Vries E. PET imaging in multiple sclerosis. J. Neuroimmune Pharmacol. 2014;4:468–82.

18. Padma MV, Adineh M, Pugar K, Mukherjee J, Satter M, Shi B, et al. Functional imaging of a large demyelinating lesion. J. Clin. Neurosci. 2005;12:176–8.

19. Matsuzono K, Deguchi K, Hishikawa N, Yamashita T, Ichikawa T, Date I, et al. Tumefactive demyelinating disease mimicking malignant tumor in positron emission tomography with ^{11}C-mithionine. Neurol Clin Neurosci. 2015;3:81–3.

20. Maeda Y, Oguni H, Saitou Y, Mutoh A, Imai K, Osawa M, et al. Rasmussen syndrome: multifocal spread of inflammation suggested from MRI and PET findings. Epilepsia. 2003;44:1118–21.

21. Morooka M, Kubota K, Minamimoto R, Furuhata M, Abe T, Ito K, et al. ^{18}F-FDG and ^{11}C-methionine PET/CT findings in a case with anti-NMDA (NR2B) receptor encephalitis. Clin Nucl Med. 2012;37:400–2.

22. Hirata K, Shiga T, Fujima N, Manabe O, Usui R, Kuge Y, et al. ^{11}C-Methionine positron emission tomography may monitor the activity of encephalitis. Acta Radiol. 2012;53:1155–7.

23. Tsuyuguchi N, Sunada I, Ohata K, Takami T, Nishio A, Hara M, et al. Evaluation of treatment effects in brain abases with positron emission tomography. Ann Nucl Med. 2003;17:47–51.

24. Uda T, Tsuyuguchi N, Terakawa Y, Takami T, Ohata K. Evaluation of the accumulation of ^{11}C-methionine with standardized uptake value in the normal brain. J Nucl Med. 2010;51:219–22.

25. Clatterbuck RE, Eberhart CG, Crain BJ, Rigamonti D. Ultrastructural and Immunocytochemical evidence that an incompetent blood-brain barrier is related to the Pathophysiology of cavernous malformations. J Neurol Neurosurg Psychiatry. 2001;71:188–92.

26. Naito K, Yamagata T, Arima H, Abe J, Tsuyuguchi N, Ohata K, et al. Qualitative analysis of spinal intramedullary lesionsusing PET/CT. J Neurosurg Spine. 2015;23:613–9.

27. Planas AM, Prenant C, Mazoyer BM, Comar D, Di Giamberardino L. Regional cerebral L-[^{14}C-methyl]methionine incorporation into proteins: evidence for methionine recycling in the rat brain. J Cereb Blood Flow Metab. 1992;12:603–12.

28. Glaudemans AW, Enting RH, Heesters MA, Dierckx RA, van Rheenen RW, Walenkamp AM, et al. Value of ^{11}C-methionine PET in imaging brain tumours and metastases. Eur J Nucl Med Mol Imaging. 2013;40:615–35.

29. Ninomiya S, Hara M, Morita A, Teramoto H, Momose M, Takahashi T, et al. Tumefactive demyelinating lesion differentiated from a brain tumor using a combination of magnetic resonance imaging and ^{11}C-methionine positron emission tomography. Intern Med. 2015;54:1411–4.

30. Schiepers C, VanHecke P, Vandenberghe R, Van Oostende S, Dupont P, Demaerel P, et al. Positron emission tomography, magnetic resonance imaging and proton NMR spectroscopy of white matter in multiple sclerosis. Mult Scler. 1997;3:8–17.